IEEE Access
Multidisciplinary | Rapid Review | Open Access Journal

Received November 12, 2018, accepted December 7, 2018, date of publication December 21, 2018,
date of current version January 23, 2019.

Digital Object Identifier 10.1109/ACCESS.2018.2889075

Dynamic Behavior of Droplets and Flashover Characteristics for CFD and Experimental Analysis on SiR Composites

YONG LIU, (Member, IEEE), XIANGHUAN KONG, YAFENG WU, AND BOXUE DU, (Senior Member, IEEE)

School of Electrical and Information Engineering, Tianjin University, Tianjin 300072, China

Corresponding author: Yong Liu (tjuliuyong@tju.edu.cn)

This work was supported in part by the National Nature Science Foundation of China under Grant 5167718, and in part by the Science and Technology Project of the State Grid Corporation of China under Grant 5202011600UV.

ABSTRACT The dynamic mechanism of water droplet formation has recently drawn considerable attention in research and application toward silicon rubber composite insulators. This paper is aimed at numerical simulations and experiments on the dynamic mechanism of water droplet formation with different applied voltages and droplet distribution and induced surface discharges on the insulator surface under the impact of AC electric field. The computational fluid dynamics model and experimental setup of multiple droplets were established to analyze the dynamic behavior of droplets and flashover characteristics. The obtained results reveal that the fusion first occurs between larger size droplets and the fusion is hard to happen along with the rise of the fractal dimension (FD) of droplet distribution. The elongation of droplets merges with more droplets and finally affects the electric field distribution on the insulator surface. With the increase of FD, the maximum electric field intensity shows an increasing tendency. Meanwhile, the experimental results show that with the increase of electric field intensity, the droplet fusion phenomenon becomes more obvious, which is consistent with the simulation results. The flashover voltage on the surface of silicon rubber decreases with the decrease of the FD of droplets, indicating that the complexity of droplet distribution has a significant effect on the flashover voltage.

INDEX TERMS Droplet elongation, flashover voltage, discrete droplet, sir composite, fractal dimension.

I. INTRODUCTION

As is generally known, silicone rubber (SiR) composite insulators have been widely used for their excellent insulation performance, hydrophobicity and bear pollution flashover properties in coastal power grid in China [1]. Many researches have been published on the spreading behaviors of droplet under different conditions [2], [3]. These investigations can be mainly divided into two categories: one concerns the dynamic mechanism of single water droplet distortion and breakup under different conditions, such as droplet static parameter and external environment; the other is the binary droplets coalescence under the effect of electric field and other factors. Both have respectively established experimental and simulation model to investigate the water droplet elongation and coalescence under different conditions [4], [5]. Such as electric field intensity, voltage shape, droplet viscosity and size, conductivity. However, it has not formed a complete systematic investigation about spreading characteristics and surface discharges on SiR composites under the condition of increasing the water droplet quantity from single to multiple discrete water droplets due to the complexity of dynamic mechanism of water droplets elongation and surface discharges. Therefore, it is a source of increasing interest from both academics and utilities to investigate dynamic characteristics of water droplet and induced surface discharges on SiR Composites [6], [7].

As pointed in earlier investigates [8], [9], the elongation of water droplet is related to the interaction between the electric field (E-field) and hydrodynamic stresses undergo. M. H. Nazemi et al have investigated the elongation behavior of water droplet on the insulator surface at different voltage shapes (AC, DC and combined AC-DC voltages). The water droplet elongates towards different electrodes at different voltage shapes, which affects the partial discharge

inception E-field intensity [10]. A. Beroual et al have investigated the coalescence of water droplet on composite insulator surface under DC electric field. Based on the simulation analysis and experimental study, the coalescence behavior of these water droplets depends on their size, conductivity and location [11]. Li et al have performed the investigation of the electric field driven self-propelled motion of water droplets on a super-hydrophobic surface. Based on three different insulating materials (glass sample, silicone sample, super-hydrophobic sample) with distinctly different wetting properties, the behavior of water droplet is measured in an oscillating electric field by experimental and simulation methods [12]. Therefore, moisture is an important environmental factor affecting the insulation reliability of silicone rubber composite insulator in power system. The discrete water droplet can enhance electric field intensity on the insulator surface. The partial discharge may occur at triple junction of the water droplet, air and insulating material, which can accelerate degradation and aging of the insulator. Therefore, the investigation about the dynamic spreading behavior of multiple water droplets is great of importance [13]–[16].

In this paper, the dynamic process of water droplet elongation and change of flashover voltage are analyzed by using COMSOL Multiphysics software and experimental method. Effects of the electric field intensity and water droplet distribution on the water droplet elongation and flashover voltage are obtained, which is beneficial to further understand pollution flashover mechanisms of polymer insulators in coastal power grid.

II. SIMULATION MODEL AND METHOD

A. SIMULATION MODEL

Figure 1 shows the simulation model of water droplet in two-dimensional space, which is designed in form of simplified model of silicone rubber insulator surface. The dimension of simulation model is 20 mm × 10 mm. The randomly multiple water droplets generated by COMSOL Multiphysics 5.3 with MATLAB are placed on the surface of the composite insulator and are surrounded by the air. A sinusoidal alternating voltage with a frequency of 50 Hz is applied across the sample to form a homogeneous electric field on the surface of the insulator. In order to make the electric field strength of the SiR surface 15 kV/cm, the ground electrode and the high voltage electrode are respectively applied to the left and right sides of the sample. The specific values of the dielectric parameters of water and air selected in the simulation are shown in TABLE 1.

Figure 2 shows that the quantity statistics of random droplet distribution. There are 145 water droplets in the random distribution map, of which the maximum radius is 2 mm. As shown in this figure, the number of small size water droplet is 138, which accounts for the vast majority of droplets distribution. The droplet distribution follows the random principle owing to the droplet radium ratio of adjacent generations is 1.25. The result shows that the

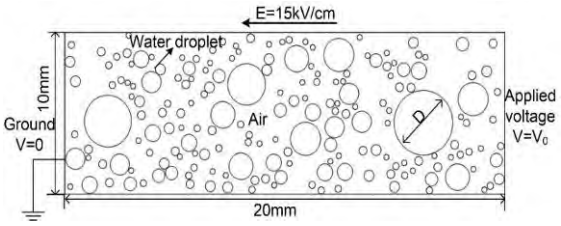

FIGURE 1. The simulation model of multiple water droplets.

TABLE 1. The dielectric parameters of water and air.

Dielectric Materials	Density (kg/m^3)	Viscosity (mPa·s)	Relative dielectric constant	Conductivity (S/m)
water	1000	1.002	81	2e-4
air	1.205	0.0181	1	1e-14

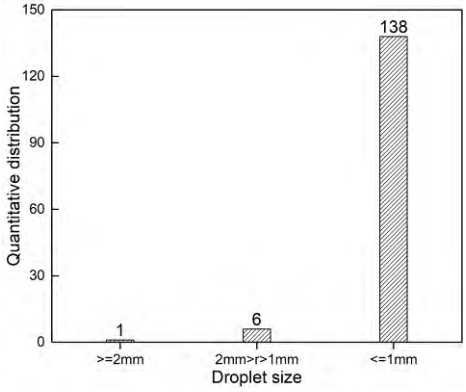

FIGURE 2. The quantity statistics of random droplet distribution.

simulation result of random droplet distribution produced by COMSOL with MATLAB is in very good agreement with experimental result represented by Burnside and Hadi [17] and Wu *et al.* [18].

B. SIMULATION METHOD

In order to study dynamic elongation characteristics of droplets under AC electric field, the droplet model under AC electric field is established using the phase field method based on Cahn-Hilliard formulation. In electro hydrodynamic, as the dynamic current is small and can be ignored. The electric field intensity $\mathbf{E}$ is irrotational ($\nabla \times \mathbf{E} = 0$), and the charge conservation equation is given by the following:

$$\nabla \cdot \boldsymbol{J} = -\frac{d\,(\nabla \cdot \boldsymbol{D})}{dt} \tag{1}$$

where $\boldsymbol{J} = \kappa \boldsymbol{E} + j\omega\varepsilon_0\varepsilon_r \boldsymbol{E}$; $\boldsymbol{J}$ is the current density; κ is the fluid conductivity; ε_0 is the permittivity of the vacuum; and ε_r is the relative dielectric constant. The Gauss law can be written ($\boldsymbol{D} = \varepsilon_0\varepsilon_r \boldsymbol{E}$) in a dielectric material, and the electric field intensity is given by the gradient of a potential function:

$$\boldsymbol{E} = -\nabla U \tag{2}$$

The interface between the water droplet and the air is a free surface that can be deformed by the Lorentz force. The electric field force tends to elongate the water droplet and is opposed by the surface tension which tends to bring back the water droplet to its equilibrium state. Due to the water droplet is a compressible fluid, the two-phase flow problem is governed by the equation of momentum and mass conservation, namely the Navier-Stokes (NS) equations, which can be expressed as follows:

$$\rho\frac{\partial \boldsymbol{u}}{\partial t}\rho(\boldsymbol{u}\cdot\nabla)\boldsymbol{u} = \nabla\cdot[-p\boldsymbol{I}+\mu(\nabla\boldsymbol{u}+(\nabla\boldsymbol{u})^T)]+\boldsymbol{F}+\rho\boldsymbol{g}+\boldsymbol{F}_{st} \tag{3}$$

$$\nabla\cdot\boldsymbol{u} = 0 \tag{4}$$

where ρ denotes the fluid density; $\boldsymbol{u}$ is the velocity vector of the fluid; μ is the dynamic viscosity; $\boldsymbol{F}$ is the electric field force; $\boldsymbol{F}_{\mathrm{st}}$ is the surface tension force; $\boldsymbol{g}$ is the acceleration of gravity. The electric force vector $\boldsymbol{F}$ is given by the divergence of the Maxwell stress tensor $\boldsymbol{T}$

$$\boldsymbol{F} = \nabla\cdot\boldsymbol{T} \tag{5}$$

The Maxwell stress tensor is given by

$$\boldsymbol{T} = \varepsilon_0\varepsilon_r\left[\boldsymbol{E}\boldsymbol{E}-\frac{1}{2}(\boldsymbol{E}\cdot\boldsymbol{E})\boldsymbol{I}\right] \tag{6}$$

The simulation model is discretized by fixed grid. Phase field method is used to capture the interfacial motion, which can be expressed as follows:

$$\frac{\partial\phi}{\partial t}+\boldsymbol{u}\cdot\nabla\phi = \nabla\cdot\chi\nabla G \tag{7}$$

where χ is mobility and the variable G can be expressed as:

$$G = \lambda\left[-\nabla^2\phi+\frac{\phi(\phi^2-1)}{h^2}\right] \tag{8}$$

As a source of Eq. (4), the relationship between interfacial tension vector (F_{st}) and G is shown as Eq. (9).

$$\boldsymbol{F}_{st} = G\nabla\phi \tag{9}$$

III. SIMULATION RESULT AND DISCUSSION

A. THE DYNAMIC BEHAVIOR OF WATER DROPLET

For better understanding the dynamic behavior of multiple water droplets on SiR surface, the model of randomly multiple droplets, which is generated by COMSOL Multiphysics with MATLAB, is investigated by changing the radius ratio of water droplets. The droplet distribution is random and irregular on the insulator surface. Hence, fractal dimension is used to extract and identify characteristics of droplet distribution based on the fractal geometry. Sarkar and Chaudhuri proposed a Differential Box-Counting (DBC) method to calculate fractal dimension of droplet distribution image [19]–[21]. If N is the number of boxes that cover the pattern, r is the box size, the fractal dimension (FD) is given by:

$$\mathrm{FD} = \frac{\log(N_r)}{\log(1/r)} \tag{10}$$

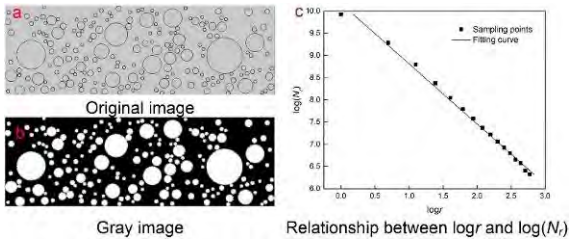

FIGURE 3. The computational method of fractal dimension.

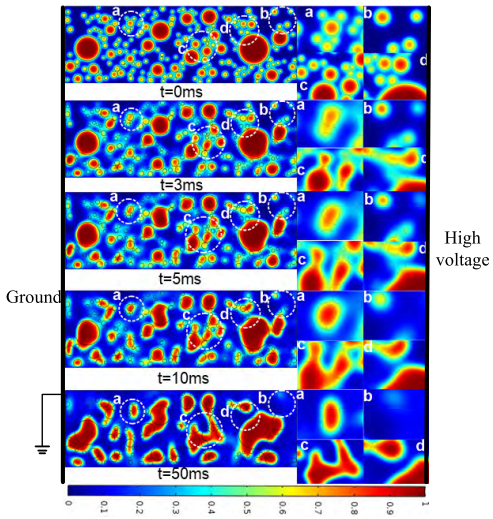

FIGURE 4. The dynamic behavior of multiple droplets at different lapse time. (I) General distribution. (II) Local magnification.

As shown in the Figure 3, original image (Figure 3(a)) is converted to gray scale and then edge detector is applied to the gray-scale image (Figure 3(b)). The fractal dimension is calculated by counting the white pixels of defined radius circle. The slope of fitting line is the FD of droplet size and quantity describing the distribution characteristics of the investigated images as shown in the Figure 3(c).

Figure 4 shows the dynamic behavior of multiple droplets at different lapse time under AC E-field intensity (15 kV/cm). Figure 4(I) is the general distribution of dynamic behavior, and figure 4(II) is the local magnification of different positions. With the increase of lapse time, water droplets moved and fused under the influence of AC E-field. When the distances of random droplets were same, droplet fusion occurred firstly between large droplets and small droplets along the E-field direction, as shown in the Figure 4(a) at 5 ms. During the fusion, there was a phenomenon that small water droplets were dragged to the side of the large water droplets. As the difference in the size of the water droplets increases, the dragging phenomenon becomes more obvious (Figure 4(c) and 4(d)). Due to the slow spreading process of large droplets, the fusion time between large droplets is longer than that between large droplets and small droplets.

Figure 5 shows that the dynamic behavior of multiple droplets under different AC E-field intensity. With the increase of applied voltage, the fusion speed and elongation

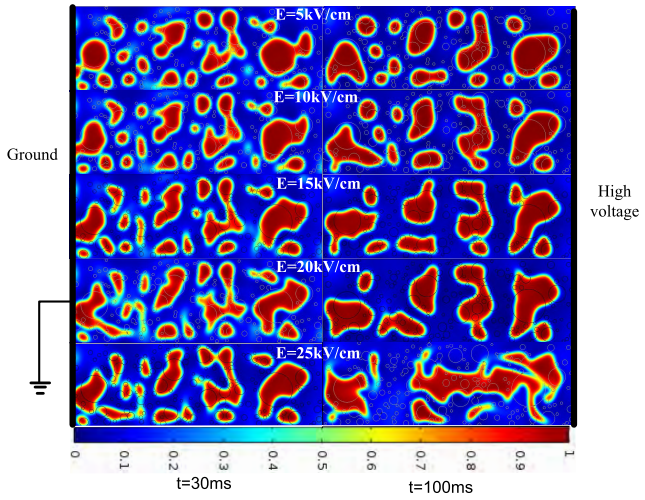

FIGURE 5. The dynamic behavior of multiple droplets under different AC E-field intensity.

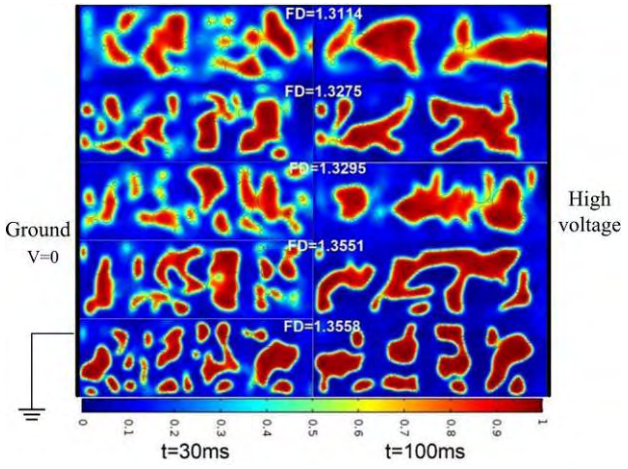

FIGURE 6. The dynamic behavior of multiple droplets under different fractal dimension.

shows an increasing tendency. The fused droplets are elongated again and finally reach a stable state under effects of E-field force. The fusion phenomenon of the droplets on the high voltage side is more obvious than that of the droplets on the low voltage side. This is mainly because the E-field force plays a promoting role in the dynamic behavior of droplet, and it shows an increasing tendency with the increase of droplet size. Therefore, the electric field force is one of the important factors affecting the elongation and fusion of droplets.

Figure 6 shows that the dynamic behavior of multiple droplets under different FD when applied voltage is 15 kV/cm. A larger value of FD indicates that the water droplets are distributed more complexly and irregularly, while a smaller value reflects a more regular distribution. As the fractal dimension of multiple droplets increases, the fusion speed shows a declining trend. This is mainly because with the increase of the dispersed phase droplet density, the stronger the molecular force acts between the dispersed

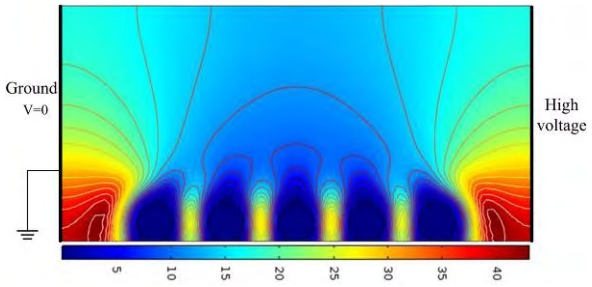

FIGURE 7. The E-field distribution under the condition of uniform droplets.

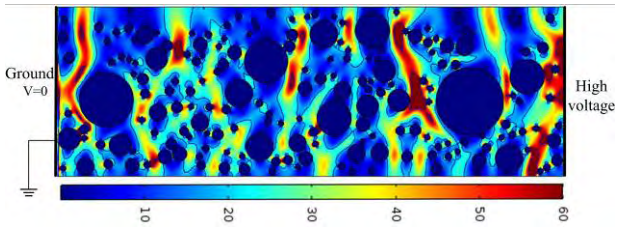

FIGURE 8. The E-field distribution under the condition of random droplets.

phase droplet, which can effectively restrict the elongation and fusion of droplets. With the increase of fractal dimension, the complexity and irregularity of droplet distribution increase significantly, which makes the fusion more difficult between different droplets.

B. THE ELECTRIC FIELD DISTRIBUTION CHARACTERISTICS

Figure 7 shows that the E-field distribution under the condition of uniform water droplets. As shown in the figure, the maximum E-field intensity on the surface of water droplets is at the junction point of surface. The internal E-field value of water droplet is approaching 0, resulting that the whole droplet can be regarded as an equipotential body. That is because the permittivity of water droplet is much larger than that of air. The droplets on the surface of the dielectric cause the electric field distribution to be distorted, resulting that the equipotential lines are densely distributed around the droplets.

Figure 8 shows that the E-field distribution under the condition of random water droplets. It is seen that the maximum E-field intensity on the sample surface is generated between the different size droplets. With the increase of irregular distribution of droplets, the electric field intensity around droplets tends to increase. That is because irregular droplets increase the complexity of the electric field, which distorts the electric field around the droplets. The distortion of E-field sharply increases near the two electrodes resulting in the occurrence of partial discharge on the insulating surface.

Figure 9 shows that the relationship between maximum E-field intensity and fractal distribution using the fitting of logistic function. With the increase of fractal distribution, the maximum E-field intensity shows an increasing tendency

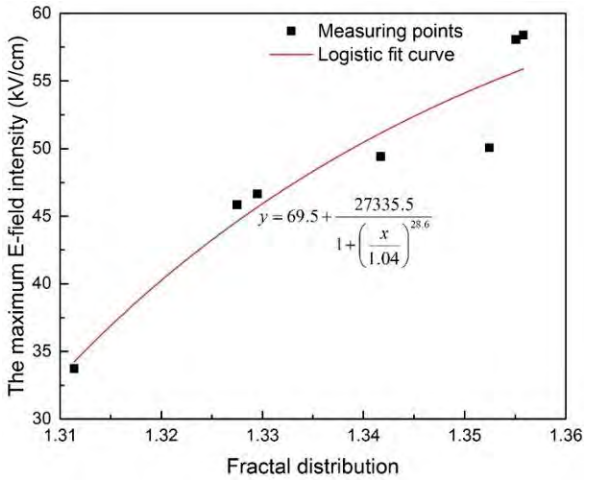

FIGURE 9. The relationship between maximum E-field intensity and fractal distribution.

with the increased speed basically keeping constant. It is considered that the increasing non-uniform distribution of droplets on the insulator surface can induce an easier occurrence of surface discharge. It is mainly because the different distributions have an effective influence on the homogeneity of E-field distribution along the specimen surface and even causing partial discharge may occur at the triple junction of the water droplet, air and the insulating materials, where the E-field reaches critical strength of air breakdown. As a result, the propagation of surface discharges will connect the partial discharge arcs to cause a flashover.

IV. EXPERIMENTAL SETUP AND RESULT

A. EXPERIMENT FACILITIES AND PROCEDURE

Figure 10 shows that the schematic diagram of experimental setup. The sample is the slice removing from SiR insulator with the dimensions of 65 mm×30 mm×5 mm, which is horizontally put on an insulation test-bed. The electrode on the surface of the dielectric is plate-plate electrode with a length of 23 mm. The plate-plate electrode is set with the parallel distance of 43 mm. The left plate electrode is connected to the high voltage (frequency 50 Hz) via a protection resistor, and the right plate electrode is connected to the ground. The experiment is conducted in a closed salt-fog chamber with dimensions of 1200 mm × 640 mm × 1125 mm. The temperature and humidity (relative humidity) of the experiment environment were respectively set at 24.8°C and 65%.

The experiment is aimed to investigate the dynamic behavior and flashover voltage of multiple droplets. The ultrasonic fog generator can produce multiple water droplets by controlling lapse time. Droplets with different sizes are condensed on the surface of sample by controlling setting time. The conductivity of the droplet generated by the ultrasonic fog generator is 2×10^{-4}S/m, which is adjusted by adding NaCl to the deionized water. After experimental setup is powered, the applied voltage is homogenously increased in small steps of about 3kV by controlling voltage regulator, and each

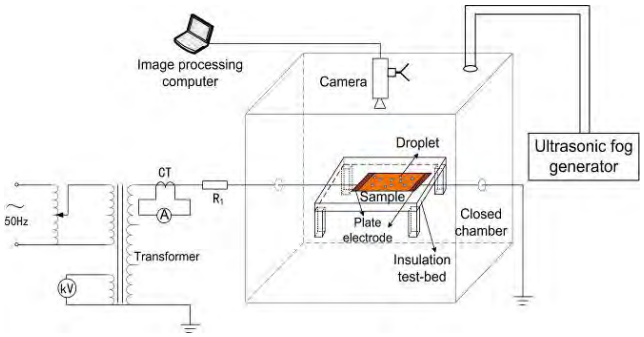

FIGURE 10. Schematic diagram of the experimental setup.

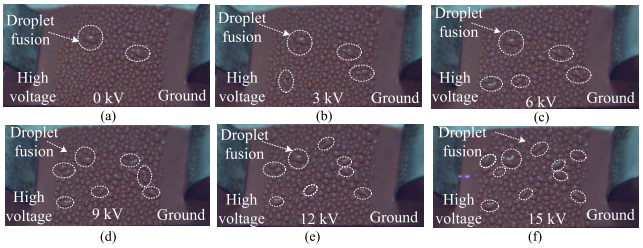

FIGURE 11. The relationship between droplets dynamic behavior and applied voltage.

voltage grade withstands 2 minutes. The dynamic behavior of water droplets under effects of AC E-field is capture by a high-speed camera with 1000 frames per second. When the flashover discharge is occurred on the insulator surface, the process of droplet discharge and droplet movement is recorded. The applied voltages at which surface discharge and flashover occurred were measured and defined as the onset voltage of surface discharge and the flashover voltage [22]–[25].

B. EXPERIMENTAL RESULTS OF MULTIPLE DROPLETS

Figure 11 shows the dynamic behavior of water droplets under effects of different applied voltage. From these figures, we can see that partial water droplets produce fusion between adjacent droplets. When the peak value of applied voltage is less than 6 kV, water droplets have not obvious changes and only oscillate periodically on the insulator surface. With the increase of applied voltage, the electric field force of water droplet overcomes surface tension to make water droplets elongate along the direction of electric field and fuse between adjacent droplets. Finally, the dynamic behavior of water droplet results in discharges or even flashover discharges on the insulator surface.

The development process of flashover of the insulator surface after applying a uniformly increasing voltage is shown in Figure 12. In this paper, the droplets dynamic behavior and the flashover development process are divided into the following six stages: (a) Due to the excellent hydrophobicity of the SiR composite, the diameter of droplet was relatively small. The droplets adhered to the insulator surface at a large contact angle so that no continuous water strips were

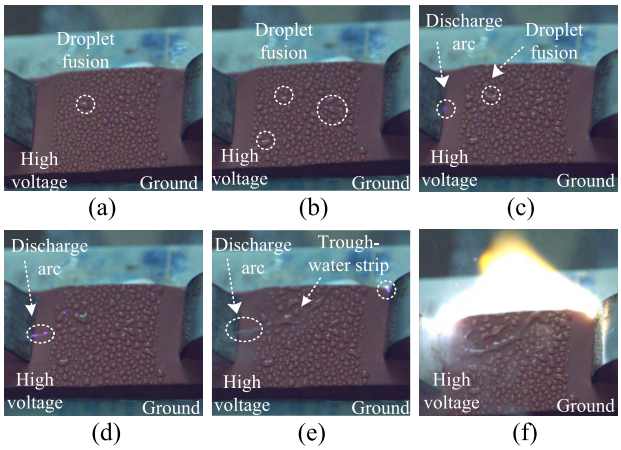

FIGURE 12. Flashover process of multiple droplets on silicone rubber surface.

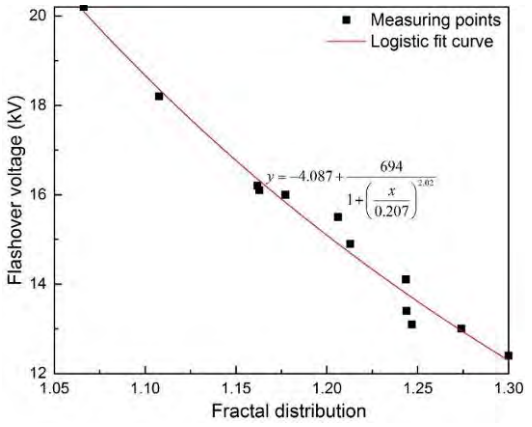

FIGURE 13. The relationship between flashover voltage and fractal distribution.

formed between each other. (b) The droplets extended under the influence of the electric field force, causing the adjacent droplets to form a larger-sized droplet. (c) The droplets on the surface of the insulator caused the distortion of the electric field. After the electric field intensity reached the breakdown strength of air, a lavender arc appeared near the high voltage electrode. (d) As the electric field intensity increase, a more severe partial discharge occurred near the high voltage electrode, resulting in a brighter purple arc. (e) The droplets were extended by the increasing electric field force, leading that the droplets between the two electrodes formed a trough-water strip. Meanwhile, blue arcs appeared near the high voltage electrode and low voltage electrode. (f) As the area of the drying zone increases and the arc develops, the arc directly penetrates the two electrodes, forming a flashover of the insulator surface.

Figure 13 shows that the relationship between flashover voltage and fractal distribution using the fitting of logistic function. As shown in this figure, there is a negative relationship between flashover voltage and fractal distribution. It is considered that when more droplets are condensed on the insulator surface and form the discrete conductive layer. The decrease in the dry-area will sustain more electrical energy, the E-field intensity at the triple of the water droplet, air and insulating materials and the air can be easily raised to the breakdown intensity of air. The arc discharge will occur in the dry bands among the layer or between the layer and the electrode. The FD value varies from 1.0 to 1.4 and shows an increasing tendency with the enhancement of lapse time, which indicates that the surface discharge becomes more complicated and irregular.

V. CONCLUSION

This paper focused on the experiment and simulation investigation on the dynamic mechanism of droplets under different conditions of E-field intensity and water droplet distribution, and induced surface discharge on SiR Composites. The main conclusions are as follows:

1) The electric field driving the elongation of water droplets on the silicone rubber insulator surface under an applied AC electric field is confirmed to be the result of the combined the electric field force and surface tension acting on water droplets.

2) The value of E-field intensity and droplet distribution have significant effects on the dynamic behavior of droplet elongation and fusion. With the increase of E-field intensity, the fusion and elongation speed show an increasing tendency. As the fractal dimension of droplets increases, droplet fusion becomes more and more difficult.

3) As the fractal dimension of the droplet increases, the maximum electric field strength around the droplet shows an increasing trend, resulting that the partial discharge easily occurs.

4) The experimental results reveal that dynamic behavior and flashover characteristics are related to electric field intensity and FD of droplets size distribution.

REFERENCES

[1] H. Ye, M. Clemens, and J. Seifert, "Electroquasistatic field simulation for the layout improvement of outdoor insulators using microvaristor material," *IEEE Trans. Magn.*, vol. 49, no. 5, pp. 1709–1712, May 2013.

[2] F. Aouabed, A. Bayadi, A. E. Rahmani, and R. Boudissa, "Finite element modelling of electric field and voltage distribution on a silicone insulating surface covered with water droplets," *IEEE Trans. Dielectr. Electr. Insul.*, vol. 25, no. 2, pp. 413–420, Apr. 2018.

[3] L. Cheng, R. Liao, L. Yang, and F. Zhang, "An optimized infrared detection strategy for defective composite insulators according to the law of heat flux propagation considering the environmental factors," *IEEE Access*, vol. 6, pp. 38137–38146, 2018.

[4] P. Yue, C. Zhou, J. J. Feng, C. F. Ollivier-Gooch, and H. H. Hu, "Phase-field simulations of interfacial dynamics in viscoelastic fluids using finite elements with adaptive meshing," *J. Comput. Phys.*, vol. 219, no. 1, pp. 47–67, Nov. 2006.

[5] H. Songoro, E. Gjonaj, and T. Weiland, "Computational modeling of water droplet elongation in strong electric fields," in *Proc. IEEE Conf Electromagn. Adv. Appl.*, Oct. 2012, pp. 333–336.

[6] C. Song, Q. Chen, X. Wang, L. Wen, and T. Zheng, "Deformation and motion behavior of droplets in a non-uniform electric field," in *Proc. IEEE 11th Int. Conf. Properties Appl. Dielectric Mater. (ICPADM)*, Jul. 2015, pp. 652–655.

[7] Y. Yan, D. Guo, and S. Z. Wen, "Dynamic behaviors of microdroplets in convergent microchannels under the effect of dielectrophoresis," in *Proc. 8th Annu. IEEE Int. Conf. Nano/Micro Engineered Mol. Syst.*, Apr. 2013, pp. 60–63.

[8] K. Adamiak and J. M. Floryan, "Dynamics of water droplet distortion and breakup in a uniform electric field," *IEEE Trans. Ind. Appl.*, vol. 47, no. 6, pp. 2374–2383, Nov./Dec. 2011.

[9] S. Chatterjee, R. K. Dholey, R. Bose, and P. Roy, "Electric field computation in presence of water droplets on a polymeric insulating surface," in *Proc. 2nd Int. Conf. Control, Instrum., Energy Commun. (CIEC)*, Jan. 2016, pp. 116–119.

[10] S. Chatterjee and M. H. Nazemi, "Influence of viscosity and conductivity of water droplets on partial discharge inception voltages of polymeric insulating surfaces," in *Proc. Int. Conf. Energy, Power Environ., Towards Sustain. Growth (ICEPE)*, Jun. 2015, pp. 1–4.

[11] J. Ndoumbe, A. Beroual, and A. M. Imano, "Simulation and analysis of coalescence of water droplets on composite insulating surface under DC electric field," *IEEE Trans. Dielectr. Electr. Insul.*, vol. 22, no. 5, pp. 2669–2675, Oct. 2015.

[12] J. Li, Y. Wei, Z. Huang, F. Wang, and X. Yan, "Investigation of the electric field driven self-propelled motion of water droplets on a super-hydrophobic surface," *IEEE Trans. Dielectr. Electr. Insul.*, vol. 23, no. 5, pp. 3007–3015, Oct. 2016.

[13] H. El-Kishky and R. S. Gorur, "Electric field computation on an insulating surface with discrete water droplets," *IEEE Trans. Dielectrics Electr. Insul.*, vol. 3, no. 3, pp. 450–456, Jun. 1996.

[14] P. Basappa, V. Lakdawala, B. Sarang, and A. Mishra, "Simulation of electric field distribution around water droplets on outdoor insulator surfaces," in *Proc. IEEE Int. Symp. Elect. Insul. Conf. Rec.*, Jun. 2008, pp. 50–54.

[15] J. Wang, X. Wen, L. Lan, and H. Liu, "Study of discharge process and characteristics of discrete water droplets on the RTV hydrophobic surface in the non-uniform electric field," in *Proc. China Int. Conf. Electr. Distrib.*, 2006, pp. 1–6.

[16] Z. Cheng, X. Liang, Y. Zhou, S. Wang, and Z. Guan, "Study of water droplet discharge by electric field computation and high-speed video," in *Proc. 7th Int. Conf. Properties Appl. Dielectric Mater.*, Jun. 2003, pp. 820–823.

[17] B. M. Burnside and H. A. Hadi, "Digital computer simulation of dropwise condensation from equilibrium droplet to detectable size," *Int. J. Heat Mass Transf.*, vol. 42, no. 16, pp. 3137–3146, Aug. 1999.

[18] Y.-T. Wu, C.-X. Yang, and X.-G. Yuan, "Drop distributions and numerical simulation of dropwise condensation heat transfer," *Int. J. Heat Mass Transf.*, vol. 44, no. 23, pp. 4455–4464, Dec. 2001.

[19] F. Barakou, D. Koukoula, N. Hatziargyriou, and A. Dimeas, "Fractal geometry for distribution grid topologies," in *Proc. IEEE Eindhoven PowerTech*, Jun./Jul. 2015, pp. 1–6.

[20] N. Sarkar and B. B. Chaudhuri, "An efficient differential box-counting approach to compute fractal dimension of image," *IEEE Trans. Syst., Man, Cybern.*, vol. 24, no. 1, pp. 115–120, Jan. 1994.

[21] J. J. Zode, P. C. Choudhari, and M. Uparkar, "Methods to determine fractal dimension to detect branch retinal vein occlusion," in *Proc. Int. Conf. Wireless Commun., Signal Process. Netw.*, Mar. 2017, pp. 67–71.

[22] A. L. Souza and I. J. S. Lopes, "Experimental investigation of corona onset in contaminated polymer surfaces," *IEEE Trans. Dielectr. Electr. Insul.*, vol. 22, no. 2, pp. 1321–1331, Apr. 2015.

[23] B. X. Du, Z. L. Ma, X. X. Cheng, and Y. Liu, "Hydrophobicity evaluation of silicone rubber insulator using PD-induced electromagnetic wave," *IEEE Trans. Dielectr. Electr. Insul.*, vol. 19, no. 3, pp. 1060–1067, Jun. 2012.

[24] M. Bouhaouche, A. Mekhaldi, and M. Teguar, "Improvement of electric field distribution by integrating composite insulators in a 400 kV AC double circuit line in algeria," *IEEE Trans. Dielectr. Electr. Insul.*, vol. 24, no. 6, pp. 3549–3558, Dec. 2017.

[25] Y. Liu *et al.*, "Identification of lightning strike on 500-kV transmission line based on the time-domain parameters of a traveling wave," *IEEE Access*, vol. 4, pp. 7241–7250, 2016.

YONG LIU (M'12) was born in Tangshan, China, in 1980. He received the M.E. and Ph.D. degrees in electrical engineering from Tianjin University, China, in 2006 and 2009, respectively. Since 2009, he has been a Lecturer and, then an Associate Professor, with the School of Electrical Engineering and Automation, Tianjin University. From 2014 to 2015, he was a Research Fellow with the NSERC/Hydro-Quebec/UQAC Industrial Chair on Atmospheric Icing of Power Network Equipment, Canada. His main research interests are ageing evaluation and performance monitoring of outdoor insulators under various atmospheric conditions.

XIANGHUAN KONG was born in Henan, China, in 1995. He received the B.Sc. degree from the Harbin University of Science and Technology, Harbin, China, in 2017. He is currently pursuing the M.S. degree in electrical engineering with Tianjin University. His research interests include optimization evaluation of insulation structure of transmission lines.

YAFENG WU was born in Anhui, China. He received the B.Sc. degree from the China University of Mining and Technology, Xuzhou, China, in 2016. He is currently pursuing the M.S. degree in electrical engineering with Tianjin University. His research interests include dielectrics and electrical insulation.

BOXUE DU (M'00–SM'04) received the M.E. degree in electrical engineering from Ibaraki University, in 1993, and the Ph.D. degree from the Tokyo University of Agriculture and Technology, in 1996. He was an Associate Professor with the Niigata College of Technology, Japan. He is currently a Professor with the Department of Electrical Engineering, School of Electrical and Information Engineering, Tianjin University, China. His main research interests are dielectric failure mechanisms of polymer insulating materials, electrical insulation technology, and partial discharge measurements. He is a member of IEEJ and a Senior Member of CSEE.